Effect of Blending on the PVME Dynamics. A Dielectric, NMR, and QENS Investigation

I. Cendoya, A. Alegría, J. M. Alberdi, and J. Colmenero*

Departamento de Física de Materiales y Centro Mixto CSIC-UPV/EHU, Facultad de Química, Universidad del País Vasco, Apdo 1072, E-20080 San Sebastián, Spain

H. Grimm and D. Richter

Institut für Festkörperforschung Forschungszentrum Jülich, D-52425 Jülich, Germany

B. Frick

Institut Laue-Langevin, BP. 156, F-38042 Grenoble, France

Received December 21, 1998; Revised Manuscript Received April 13, 1999

ABSTRACT: In this work we have investigated how the dynamics of poly(vinyl methyl ether), PVME, changes by blending with deuterated polystyrene. The experimental techniques used were dielectric spectroscopy, quasielastic neutron scattering, and ^{13}C nuclear magnetic resonance. By means of these techniques, the dynamics of the poly(vinyl methyl ether) units in the blends can be selectively investigated in a huge time range ($10^{1}-10^{-11}$ s). Two different blend compositions have been investigated. The main relaxation processes observed in this range are the secondary β-process and the segmental α-relaxation. It turns out that the β-relaxation is not affected by blending. The data analysis procedure followed by us in the case of the α-process is based on the assumption that the dynamics of the PVME segments in the blends is a superposition of dynamical processes with the same shape as that in pure PVME, but with the relaxation times distributed due to the presence of concentration fluctuations. From this analysis we found that, in the blends, and in pure PVME as well, the results obtained by means of the different techniques can consistently be described with the same set of parameters. Moreover, the temperature dependence of the distribution of relaxation times in each blend composition can be accounted for by a single, temperature-independent, Gaussian distribution of the Vogel−Fulcher temperature, T_0, the average and the variance of the distribution increasing as the PVME concentration decreases. Our results suggest that a significant number of PVME segments in the blends move faster than in pure PVME. Furthermore, our results strongly indicate that each polymer component of the blend exhibits very different α-relaxation rates, i.e., different "glass transitions". Several implications of these results concerning the usually accepted ideas of polymer blend dynamics are outlined.

I. Introduction

The dynamics of miscible polymer blends in general has been widely investigated over the past years by means of different experimental techniques (see for example refs 1−19), mainly calorimetric and spectroscopic techniques (dielectric mechanical spectroscopies and nuclear magnetic resonance methods). However, despite this experimental effort, the question of how the dynamics of a given polymer is modified by blending with another polymer is still far from a complete understanding. To get more insight into this basic problem from an experimental point of view, several questions have to be considered. First of all, it is well-known that polymers are complicated systems which display a rich variety of dynamic processes extending over more than 15 decades in the time/frequency scales and which also show different spatial scales (vibrations and torsional libration modes, side group motions, secondary relaxation, segmental dynamics, and terminal relaxation being the more characteristic ones). It is clear that such a huge time/frequency scale cannot be usually covered by a single experimental technique. Therefore, the combination of different techniques is needed. However, most of the investigations reported so far were carried out by means of only one experimental technique in each case and were mainly focused on the low-frequency range (roughly in the range $10^{-6}-10^{2}$ s) of the segmental relaxation spectrum, i.e., on the so-called α-relaxation. Likely, this was directly related to the old criterion that miscible polymer blends have to display only one glass-transition temperature, i.e., only one α-relaxation, intermediate to those of the polymer components of the blend considered. It is worth emphasizing that, according to this criterion, the α-relaxation of the two components of a miscible blend should be strongly modified by blending, finally giving rise to only one α-relaxation process in the blend. However, the α-relaxation spectrum in blends, as well as the glass transition measured by calorimetric techniques, shows a broad feature which makes it very difficult to distinguish whether only one broad α-relaxation or two separate and broad processes are present in the experimental curves. Concerning the effect of blending on dynamic processes other than the α-relaxation, there are only a few investigations reported.[7,9,12,17] The experimental results currently available seem to indicate that the faster and the more localized a molecular motion is, the less it would be affected by blending. For example, it has recently been shown by quasielastic neutron scattering[17] that the methyl group rotation of poly(vinyl methyl ether) is hardly sensitive to blending with polystyrene, even for blends with 80 wt % of polystyrene. However, the generalization of those results needs the input from new high-frequency experi-

10.1021/ma9819539 CCC: $18.00 © 1999 American Chemical Society
Published on Web 05/19/1999

mental data on different polymer blend systems. On the other hand, it is worth emphasizing that, as mentioned above, most of the reported investigations about polymer blend dynamics have been carried out by means of calorimetric and spectroscopic techniques which do not allow to obtain information about the spatial scales (geometry) of the molecular motions involved. This information is of the utmost importance in order to understand polymer dynamics in blends from a microscopic point of view. It is well-known that there is currently only one technique that allows to get insight into the geometry of the molecular motions in polymers in a spatial scale of the order of a few angstroms. This is the quasielastic neutron scattering technique. By means of this technique, the spatial information is obtained from the momentum transfer dependence of the experimental magnitudes characterizing the dynamics. It is worth noting that the time scale covered by quasielastic neutron scattering techniques extends roughly from 10^{-13} to 10^{-7} s. Finally, another important experimental question trying to face the problem of polymer blend dynamics in general is how to experimentally isolate the dynamic response of one of the two components of the blend. This is for instance of the utmost importance in order to clarify the above-mentioned basic question of whether there is only one or two separated α-relaxations (glass transitions). Experimentally, this can only be solved by using "selective experimental methods", which, in the case of spectroscopic techniques, is not always possible. For example, selectivity is only possible by means of dielectric spectroscopy when the two components of a given blend have very different molecular dipole moments. In this case, the dielectric relaxation response is dominated by the component showing the strongest dipole moment. ^{13}C nuclear magnetic resonance (NMR) also allows to selectively investigate the dynamics of each component if the resonance lines of the two component do not overlap. By means of selective isotopic labeling in combination with two-dimensional deuteron exchange 2D-NMR the dynamics of each species in a blend can also be observed, but in this case only in the low-frequency range. However, quasielastic neutron scattering techniques always allow to investigate the component dynamics of a given polymer blend by using partially deuterated systems. Due to the very different scattering cross sections of hydrogen and deuterium, if one of the components is fully deuterated and the other protonated, the neutron scattering intensity is dominated by the incoherent scattering of the hydrogen atoms. Therefore, the dynamics of the protonated polymer in the blend determines the features of the incoherent neutron scattering spectra.

On the other hand, from a theoretical point of view, the proposed models[3,6,20−22] have been focused on the question of the α-relaxation (glass transition). The basic idea behind these approaches is that the concentration fluctuations (CF), which relax much slower than the α-relaxation, produce a distribution of α-relaxation processes in the blend. This distribution should explain the broadening of the α-relaxation spectrum usually observed in blends. The distribution of α-relaxation processes can be modeled by distributing the different magnitudes involved in the α-relaxation, namely, the relaxation time and/or the nonexponentiality parameters (for example, the β-parameter of a stretched exponential representation of the α-relaxation function). The application of the coupling model proposed by Ngai to the polymer blend dynamics[23] assumes that the distribution of CF should give rise to a distribution of β values which, in the framework of the coupling model, also implies a distribution of the relaxation times throughout the, so-called, "second universality". However, from a phenomenological point of view, the β values of different polymers are rather close (apart from a few exceptions).[24] This would suggest that a good approximation should consider only a distribution of the relaxation times in particular when there are no particular specific interactions between the two homopolymer components. This has been the point of view taken in several investigations.[6,10,16,20−22] Moreover, in this latter framework it is usually also assumed that the connection between concentration fluctuations and distribution of relaxation times is through a distribution of glass-transition temperatures, each of them associated with a subvolume of the sample characterized by a given average concentration. It is worth emphasizing that this second step is based on the idea that a blend of a given concentration displays only one (although more or less broad) glass-transition process; i.e., as has been mentioned above, both components of the blend have completely homogeneous behavior concerning the α-relaxation. However, this is a question which is not completely clear from the experimental point of view. There has even been at least a clear case reported[4,5,22,25,26] where a well-known miscible system polyisoprene/poly(vinyl ethylene) seems to show different α-relaxation processes by different techniques and at different blend compositions. Taking into account this experimental result, a generalization of the CF model[20] has recently been proposed by Kumar et al.[27] and incorporates the concept of cooperativity volumes which depend on the local composition.

To contribute to the above-mentioned open questions, in this work we report on the effect of blending on the dynamics of poly(vinyl methyl ether) (PVME) over a very wide time range ($10^{1}-10^{-11}$ s). Pure PVME and two miscible polymer blends of deuterated polystyrene (dPS) with PVME have been investigated. The experimental techniques used were dielectric relaxation (DR) spectroscopy ($10-10^{-10}$ s), ^{13}C NMR ($\sim 10^{-9}$ s), and quasielastic neutron scattering (QENS) ($10^{-9}-10^{-11}$ s). In the polymer blend samples, both the strength of the dielectric relaxation and the scattering cross section of PVME units are much higher than the ones corresponding to dPS; therefore the blend dynamics, as observed by DR and QENS, is dominated by the PVME segments. Moreover, well above T_g, the ^{13}C NMR spectra of the blends show well-resolved peaks corresponding to the main-chain PVME carbons, so it also allows to selectively investigate the dynamics of the PVME segments in the blends. The chosen system has the advantage that, from earlier results in pure PVME,[28] we know that the segmental dynamics in this polymer shows "universality" in the sense that results from different techniques, like DR, NMR, and QENS, can consistently be described with the same set of parameters. The analysis of the data from the different experimental techniques followed by us is based on the idea that the main effect of the CF is to give rise to a distribution of relaxation times, the distribution of β values, if any, being negligible. However, we deduce the distribution of relaxation times directly from the experimental data without taking any "a priori" model for the connection

Table 1. Comparison of the Different Parameters Characterizing the Segmental Dynamics of the Samples Investigated[a]

PVME content (%)	T_g (K)	T_0 (K)	B (K)	τ_∞ (s)	$\langle T_0 \rangle$ (K)	σ_{T_0} (K)
100	249	200	1505	9×10^{-14}		
65	265	212	1505	9×10^{-14}	212	10.5
50	278	221	1505	9×10^{-14}	219	14.4
0 (dPS)	370	326	1272	3×10^{-13}		

[a] The parameters for the 0% PVME content are those obtained from pure dPS.

between CF and the distribution of relaxation times.

The main objectives of this work are the following: First, to investigate the PVME segmental dynamics on blends of PVME and dPS over a very wide temperature/frequency range in order to compare the results with the previous findings, which were obtained close T_g and within a rather limited frequency range. Second, to check whether in the blends the results for the dynamics of the PVME segments can again be consistently interpreted for the different techniques ("universality"). Finally, we would like to shed new light on the question of the origin of the distribution of relaxation times in polymer blends and to discuss the usual assumption of dynamic homogeneity in each subvolume (only one broad glass transition/α-relaxation for a given concentration). From that investigation we try to gain insight not only about the polymer blend dynamics but also on the segmental dynamics of polymeric systems in general.

The paper is organized as follows: In the next section we present the experimental details concerning the samples and the techniques used. In section III the raw results are depicted, and in section IV the methods for the analysis of the different experimental data in a common framework are established. In section V the results obtained from that analysis as well as a comparison among the parameter values obtained from the different techniques are presented. A discussion of the present findings in comparison with the current ideas on polymer blend dynamics is drawn in section VI, and finally, in section VII the conclusion of the present work and its implications are summarized.

II. Experimental Section

a. Samples. Deuterated polystyrene (dPS) and protonated poly(vinyl methyl ether) (PVME) were obtained from Polymer Laboratories and Aldrich Chemical, respectively. Two polymer blends containing 65 wt % PVME and 35 wt % dPS (PVME65) and 50 wt % PVME and 50 wt % dPS (PVME50) were prepared by dissolving the two components in toluene and by casting from the solution. The blend films were maintained at 80 °C under vacuum conditions for 72 h to remove the solvent completely. A reference PVME sample was prepared in a similar way. The calorimetric glass transition temperatures T_g of the blend and pure PVME were determined by means of a Perkin-Elmer DSC4 differential scanning calorimeter on samples of about 10 mg (see Table 1). The T_g values were calculated from the middle point of the DSC scans at 10 K/min on samples previously cooled from 370 K at the same rate. The T_g values found (see Table 1), which were similar to the previously reported,[29] indicated the miscibility of the blends. The phase separation temperature of the blends was about 440 K, which define the upper limit of the investigated temperature range.

b. Dielectric Relaxation Measurements. Dielectric measurements were performed on two different setups supplied by Novocontrol GmbH. For the frequency range from 10^{-2} to 10^7 Hz the setup consisted of a Solartron-Schlumberger frequency response analyzer SI 1260 supplemented by a high-impedance preamplifier of variable gain. For the frequency range from 10^6 to 10^9 Hz a Hewlett-Packard impedance analyzer HP4191A was used. For both ranges the sample was kept between two condenser plates (gold-plated electrodes, 20 and 5 mm diameter, respectively) that were maintained at a fixed distance. Frequency sweeps were performed at constant temperature with a temperature stability better than 0.05 K. The temperature range investigated was 150−430 K.

c. Nuclear Magnetic Resonance. Nuclear magnetic resonance (NMR) experiments were carried out by means of a Varian VXR-300 spectrometer on the sample melts placed in a 10 mm probe. The ^{13}C spin−lattice relaxation times, T_1, corresponding to the PVME main-chain carbons in the temperature range 350−430 K, where the different spectral lines are well-resolved, were measured at 75.4 MHz by using the technique of proton noise decoupling. The value of the spin−lattice relaxation time at each temperature was determined from exponential regression of the magnetization as a function of the recovery time.

d. Neutron Scattering Measurements. Quasielastic neutron scattering (QENS) measurements were carried out by means of the high-resolution backscattering spectrometers: IN10 at the Institute Laue Langevin (ILL) in Grenoble, France, and BSS at the Institut für Festkoerperforschung (IFF) Forschungszentrum in Jülich, Germany. The wavelength of the incident neutrons was set to $\lambda = 6.28$ Å, resulting in an energy resolution of 1 μeV (full width at half-maximum). The range of momentum transfer, Q, covered was $0.1\ \text{Å}^{-1} < Q < 2\ \text{Å}^{-1}$. The sample films of 0.1−0.5 mm thickness were placed in aluminum flat containers providing transmissions in the range 85−95%. The resolution of the spectrometer was determined by measuring the samples at 2 K. The efficiency of the detectors was determined by measuring a standard vanadium sample.

The QENS spectra were recorded at different temperatures in the range from 350 to 430 K. The raw data were corrected for detector efficiency, sample container, and absorption using standard programs. The multiple scattering effects from the proposed model scattering function were determined using the DISCUS program.[30]

III. Results

a. Dielectric Relaxation. Figures 1 and 2 show a comparison between the dielectric relaxation behavior of pure PVME and the blends, above and below T_g, respectively. Above T_g, as can be seen in Figure 1, two relaxation processes are apparent: a main loss peak at low frequencies, which depends strongly on temperature and corresponds to the segmental dynamics (α-relaxation), and a weaker, much less temperature-dependent high-frequency peak, corresponding to a secondary relaxation process. By comparing pure PVME with the blends, it is apparent that the segmental dynamics is strongly affected by blending, in contrast to the secondary relaxation. In particular, the main loss maxima of the blends are shifted toward lower frequencies, indicating a slowing down of the PVME dynamics by the presence of the stiffer dPS chains. Moreover, the main loss peak, which is markedly skewed toward high frequencies for pure PVME, is broader and more symmetric in the blends. Close to T_g, the loss peaks of the blends are even skewed toward the low frequencies particularly for the PVME50 blend. In addition to these effects, in the very low frequencies the contribution of the sample conductivity is present in all cases.

On the other hand, below the T_g value of pure PVME (Figure 2) only the secondary relaxation processes, which are present in the three samples, are observed in the frequency window investigated. From the results shown in Figure 2, it is evident that neither the position

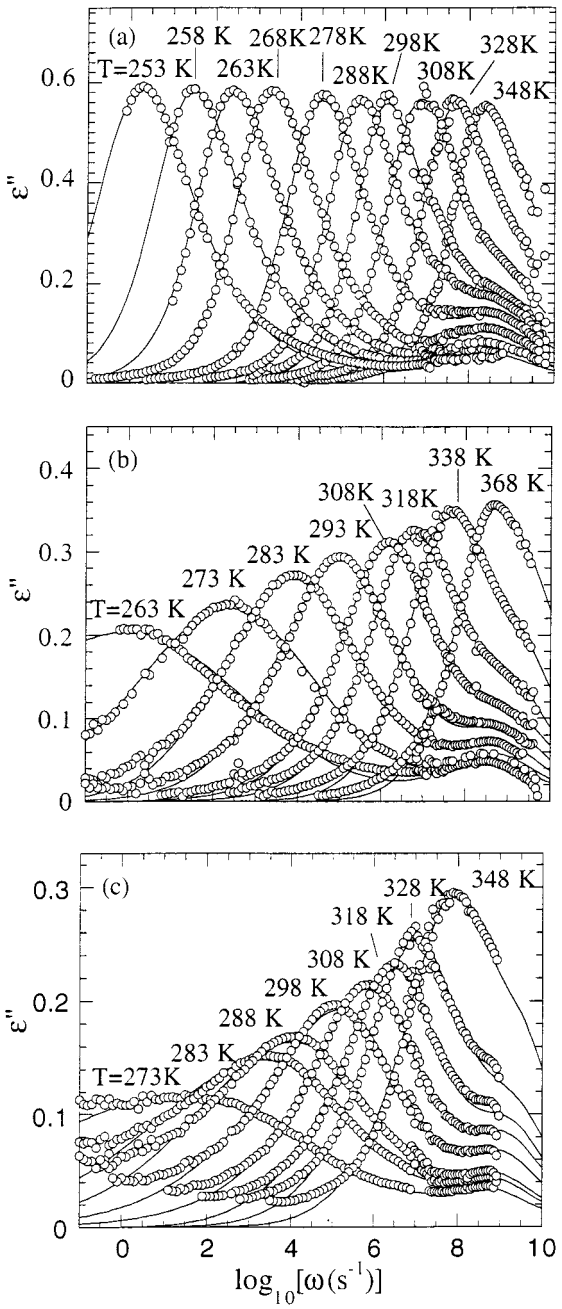

Figure 1. Dielectric loss curves at several temperatures above T_g for pure PVME (a), PVME65 (b), and PVME50 (c). The solid lines are the fitting curves according to the analysis described in the text.

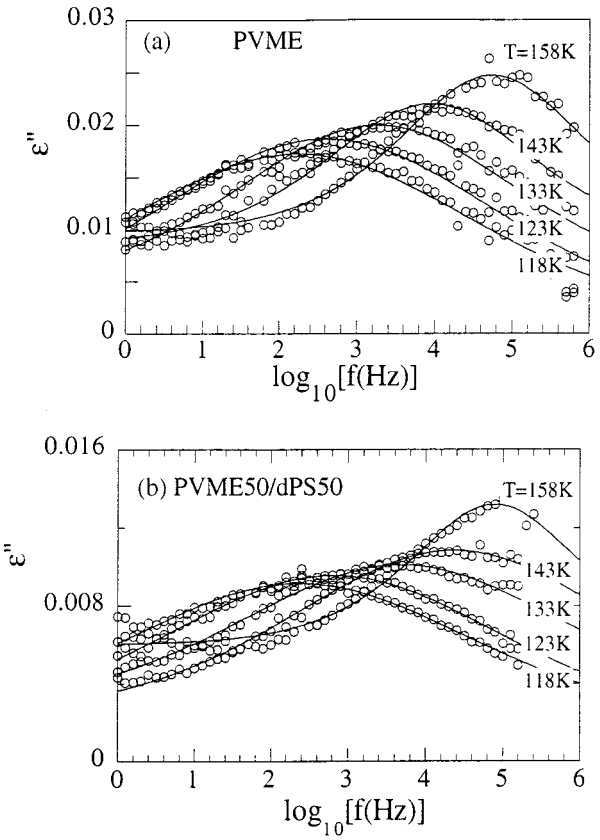

Figure 2. Dielectric loss curves at several temperatures below T_g for pure PVME (a) and PVME50 (b). The solid lines are the fitting curves corresponding to a Gaussian distribution of activated Debye-processes.

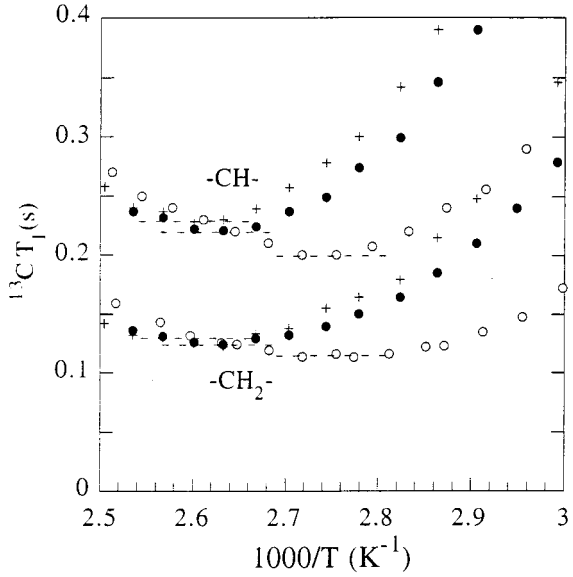

Figure 3. ^{13}C spin−lattice relaxation times of the main-chain carbons of PVME monomeric unit in pure PVME (○), PVME65 (●), and PVME50 (+).

of the loss peak nor the shape is modified by blending, when compared at the same temperature, beyond the experimental uncertainties.

It is noteworthy that although our findings in the T_g range (in the frequency range from 10^{-2} to 10^6 Hz) agree with the previously reported results,[2] the existence of a secondary relaxation in PVME and the possible effects of blending on it have not been reported so far. This fact is mainly relevant in the data evaluation of the high-temperature data where both processes seem to merge.

b. Nuclear Magnetic Resonance. Figure 3 shows the ^{13}C spin−lattice relaxation times, T_1, of the main chain carbons of PVME monomer in pure PVME and in the blends. The temperature range for this technique is limited in the low-temperature side because the resonance lines of the nonequivalent carbons are not well-resolved in this range. In the samples investigated here, this restricts the measurable temperature range to roughly $T > T_g + 50$ K. As can be shown in Figure 3, the three samples show clear minima of T_1 in the temperature range investigated. It is apparent that the T_1 minimum for the two main chain carbons is located at a similar temperature for each sample. This indicates that both carbons are involved in the same dynamical process (the segmental dynamics). We also found that

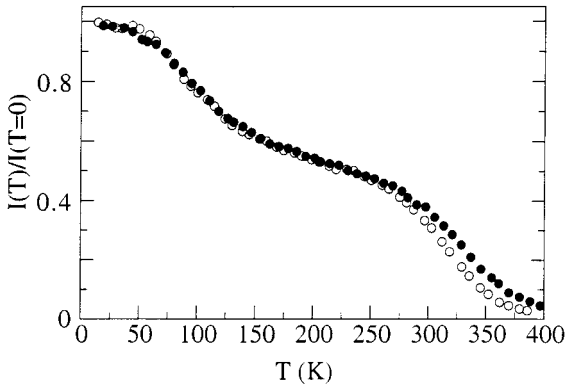

Figure 4. Neutron scattering measurements using the fixed elastic window technique at $Q = 1.93$ Å^{-1} on pure PVME (○) and PVME65 (●).

for the three samples the T_{1min} values are clearly higher than what one expects on the basis of a single-exponential relaxation, i.e., about 0.12 s for CH and 0.06 s for CH_2. Furthermore, the T_{1min} values for the blends are higher than for PVME, which indicates a broader relaxation spectrum for the blends. When comparing the minima of the blends with pure PVME, it is also apparent that the dynamics of the PVME units is slowed down by blending with dPS; thus, the values of T_{1min} occur at higher temperatures in the blends. In all three samples the T_1 minima are located at about 110−120 K above T_g.

c. Quasielastic Neutron Scattering. To have a first estimate of the effect of blending on the dynamics of PVME as observed by means of neutron scattering, we performed fixed elastic window (FEW) temperature scans in both pure PVME and the PVME65 blend. In this technique, one measures the elastic intensity as a function of the temperature. However, it is noteworthy that what is considered as elastic intensity depends on the resolution of the spectrometer and for IN10 and BSS corresponds to a characteristic time of around 10^{-8} s. Thus, roughly speaking, the scattering of the particles (protons mainly) moving slower than the characteristic time of the spectrometer is seen as elastic, whereas a decrease of the elastic intensity is observed for scattering from sample particles which move faster. When there are no motions other than vibrations, increasing the temperature, one finds a nearly linear decrease of the logarithm of the elastic intensity. However, if a relaxation process occurs within the dynamical range of the instrument, a steplike decrease in intensity should be observable.

Figure 4 shows the FEW data for both pure PVME and the PVME65 blend at $Q = 1.93$ Å^{-1}. Here the elastic intensities are normalized to their values at $T \sim 2$ K. A two-step decrease in the intensity, superimposed on a continuous decay, is clearly observed for both samples. It has been shown that the first step at low temperatures corresponds to the PVME methyl group (MG) rotation in a 3-fold potential,[31] whereas the decrease at temperatures above the glass transition is a signature of the main-chain PVME segmental dynamics. No significant differences are observed between the two samples at low temperatures, which indicates that the MG dynamics is hardly affected by blending.[17] On the contrary, a clear effect is observed in the temperature range where the segmental dynamics is detected. The major effect is a shift of the intensity step toward high temperatures, which is a clear signature of the slowing

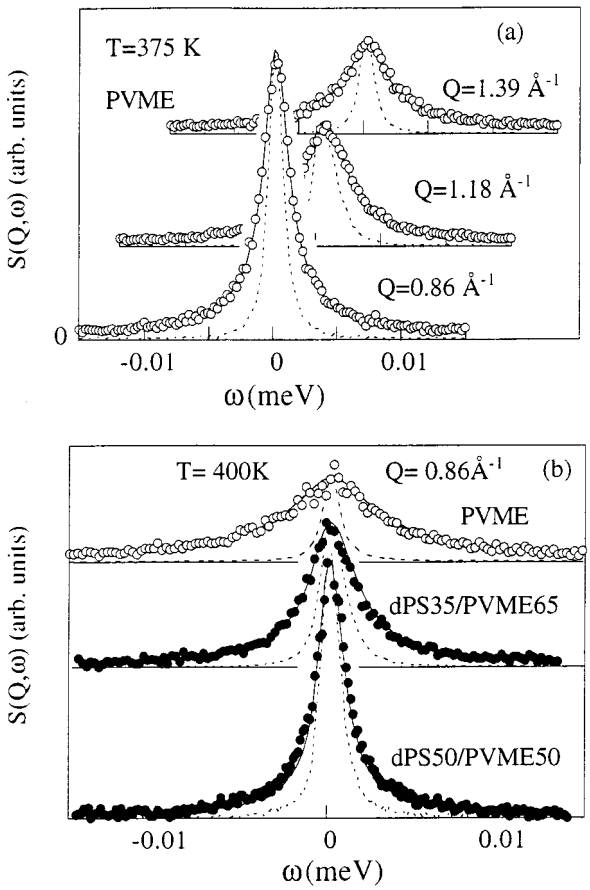

Figure 5. (a) Neutron scattering spectra of pure PVME at different Q values. (b) Effect of blending on the QENS spectra reflecting the dynamics of the PVME segments. The solid lines correspond to the fitting curves obtained with the analysis described in the text and the dashed lines to the instrumental resolutions.

down of the PVME segmental dynamics by blending also in the high-frequency range explored by QENS.

To investigate in detail the effect of blending on the PVME segmental dynamics, the spectra of pure PVME and the blends were measured at temperatures well above T_g. A clear broadening, which increases strongly with Q, is observed in the three samples at temperatures above $T_g + 100$ K. Some of the obtained results are shown in Figure 5. The shape of the respective experimental curves is hardly distinguishable by simple inspection although it is apparent that at given temperature and Q value the broadening of the spectrum is markedly reduced by blending. However, the spectra obtained for pure PVME at a given temperature are similar to those of the blends at higher temperatures (e.g., compare the spectrum obtained at $Q = 0.86$ Å^{-1} for PVME at $T = 375$ K with that for the PVME65 blend at $T = 400$ K). This result is in agreement with the T shift observed in the FEW scans shown above.

IV. Data Evaluation

As has been shown above, the dynamical processes in PVME that are faster than the segmental dynamics are not significantly affected by blending in the frequency range covered. The MG dynamics seems to be faster than the segmental dynamics at these high temperatures (it passes through the elastic window at much lower temperatures), but the dielectric secondary relaxation overlaps with the segmental dynamics at

temperatures a few tens of degrees above T_g (see Figure 1). Therefore, for the analysis of the segmental dynamics as observed by dielectric spectroscopy, a full characterization of the secondary relaxation in both samples will be essential. In this section we will establish the assumptions made for the analysis of the data obtained by means of the different experimental techniques in a common framework.

a. Secondary Relaxation. The secondary relaxations of both pure PVME and the blends, which are measurable by means of DR, have been described as the superposition of Debye-like thermally activated processes distributed according to a Gaussian distribution of activation energy barriers, i.e.

$$\epsilon_2''(\omega) = \Delta\epsilon_2 \frac{1}{\sqrt{2\pi}\sigma_E}\int_0^\infty \exp\left[-\frac{(E-E_0)^2}{2\sigma_E{}^2}\right] \times \frac{\omega\omega_m(E)}{[\omega_m(E)]^2+\omega^2}\,dE \quad (1)$$

where $\epsilon_2''(\omega)$ represents the dielectric losses associated with the secondary relaxation, $\Delta\epsilon_2$ is the corresponding dielectric relaxation strength, E_0 is the average activation energy, $\sigma_E{}^2$ is the variance of the activation energy distribution, and $\omega_m(E)$ is the relaxation rate of the process with activation energy E, i.e.,

$$\omega_m(E) \propto \exp\left(-\frac{E}{k_B T}\right) \quad (2)$$

Thus, the secondary relaxation at each temperature will be characterized by three independent parameters: $\Delta\epsilon_2$, $\omega_0 = \omega_m(E_0)$ (the angular frequency at the maximum of the loss peak), and σ_E which determines the broadening of the loss peak. When fitting the experimental dielectric loss data below T_g, we found that a weak extra contribution in the low-frequency side, likely related to the segmental dynamics, has to be considered. To account for this contribution, we used a power law.

b. Segmental Dynamics. *1. Pure Polymer.* The time decay of the relaxation function corresponding to the segmental dynamics of polymer melts is not a single exponential.[32] Although various mathematical expressions that describe the experimental data rather well have been proposed so far,[33] the Kohlrausch−Williams−Watts (KWW) function[34] is the best approximation of the relaxation function in the vicinity of the loss peak maxima having a single parameter for the shape of the relaxation function. Thus, for the PVME homopolymer, the segmental dynamics was characterized assuming a KWW function for the normalized relaxation function, i.e.

$$\varphi_H(t) = \exp\left[-\left(\frac{t}{\tau}\right)^\beta\right] \quad (3)$$

where τ is a characteristic relaxation time and $0 < \beta < 1$ measures the nonexponentiality of the relaxation process ($\beta = 1$ corresponds to a single Debye process). Since the experimental data were measured in the frequency domain, the KWW cannot be used directly, except if the Fourier transform of the data is performed, which would be affected by the cutoff effects inherent to measurements in a limited frequency range. Instead, we used the frequency domain relaxation function:

$$\Phi_H^*(\omega) = \frac{1}{[1+(i\omega/\omega_p)^\alpha]^{\gamma(\alpha)}} \quad (4)$$

with $\gamma(\alpha) = 1 - 0.812(1-\alpha)^{0.387}$, which has the form of the Havriliak−Negami equation but with a single independent parameter α for the relaxation shape, ω_p characterizing the relaxation rate. It has been shown that eq 4 is a good approximate in frequency for the KWW time function.[35−38] The parameters in eq 4 are directly related with those of the KWW function as follows:[35]

$$\beta = [\alpha\gamma(\alpha)]^{1/1.23} \quad (5)$$

$$\log\tau = -\log\omega_p - 2.6(1-\beta)^{0.5}\exp(-3\beta) \quad (6)$$

Thus, in the fitting procedure of the dielectric α-relaxation of pure PVME, we will have two parameters to describe the segmental dynamics of the homopolymer and one more to account for the relaxation strength.

2. Polymer Blends. As aforementioned, the effects of blending on the segmental dynamics have been interpreted on the basis of the dynamical heterogeneities produced by the concentration fluctuations. In the analysis of the segmental dynamics of the blend samples, we have considered the presence of dynamical heterogeneities by assuming that the contribution of the PVME segmental dynamics to the response of the blend results from a superposition of different responses, each of them given by the KWW function with the same spectral shape as the one observed in pure PVME (same value of β or α) but with the characteristic times (τ or $\omega_p{}^{-1}$) distributed due to the fluctuations of the local concentration. The assumption of no effect of blending on the relaxation shape of each process in the distribution is supported by the fact that the values of β of the two components are very similar. For example, we have found that the values of β obtained from dielectric relaxation measurements in the range from T_g to T_g + 50 K increase from 0.40 to about 0.5 in both polymers. Therefore, a significant effect of blending on the relaxation shape of each process in the distribution is hardly expected.

The basic idea of our approach is that any change in the local concentration should produce a change of the local diffusivity and therefore a different characteristic relaxation time. However, contrary to previous treatments based on the same grounds,[6,20,21] no assumption about the way the characteristic time and the local concentrations are related to each other has been made. On the basis of this general framework, the contribution of the PVME segmental dynamics to the time domain decay function of the blend can be written as

$$\varphi_B(t) = \int_{-\infty}^{\infty} g(\log\tau)\exp\left[-\left(\frac{t}{\tau}\right)^\beta\right] d(\log\tau) \quad (7)$$

or equivalently, in frequency domain, as

$$\Phi_B^*(\omega) = \int_{-\infty}^{\infty} g(\log\tau)\frac{1}{[1+(i\omega/\omega_p(\tau))^\alpha]^{\gamma(\alpha)}} d(\log\tau) \quad (8)$$

where $\varphi_B(t)$ and $\Phi_B^*(\omega)$ represent the normalized relaxation functions describing the contribution of the PVME segmental dynamics to the response of the blend sample and $g(\log\tau)$ is the distribution of KWW relaxation times associated with the fluctuations in the local

concentration. According to the aforementioned assumptions, the shape parameter β (or α) is assumed to be that found in pure PVME; thus, the dynamics of the PVME segments in the blend is uniquely characterized by the distribution function of KWW relaxation times $g(\log \tau)$.

c. Evaluation of the Dielectric Losses. According to the analysis proposed above, the different experimental quantities measured in this work can be directly evaluated from the corresponding frequency domain relaxation function $\Phi_H^*(\omega)$ for pure PVME and $\Phi_B^*(\omega)$ for the blends. In the following equations we will use $\Phi^*(\omega)$ instead of $\Phi_H^*(\omega)$ or $\Phi_B^*(\omega)$ when the corresponding equation applies indistinctly to both the homopolymer and the blends.

For dielectric measurements, the total dielectric losses of the sample can be evaluated as

$$\epsilon''(\omega) = \Delta\epsilon_1 \, \mathrm{Im}[-\Phi^*(\omega)] + \epsilon_2''(\omega) \tag{9}$$

where $\Delta\epsilon_1$ corresponds to the dielectric strength associated with the dynamics of the PVME segments in the system and, as previously mentioned, $\epsilon_2''(\omega)$ reflects the contribution of the secondary relaxation to the whole dielectric losses. In eq 9, the extremely weak contribution of the dPS dynamics to $\epsilon''(\omega)$ of the blends has been neglected.

d. Evaluation of the ^{13}C NMR Spin−Lattice Relaxation Times. For ^{13}C NMR, by assuming a purely ^{13}C−^{1}H dipolar relaxation mechanism, one finds that the T_1 values corresponding to the PVME main chain carbons are given by[39]

$$\frac{1}{nT_1} = \frac{\hbar^2 \gamma_C^{\,2} \gamma_H^{\,2}}{10 r_{CH}^{\,6}} [3J(\omega_C) + 6J(\omega_H + \omega_C) + J(\omega_H - \omega_C)] \tag{10}$$

being $J(\omega)$ the so-called spectral density which, on the assumption that for the main-chain protons of PVME the C−H bond reorientation is mainly driven by the segmental dynamics of the PVME chain, can be calculated as

$$J(\omega) = \frac{1}{\omega} \mathrm{Im}[-\Phi^*(\omega)] \tag{11}$$

In eq 10, n is the number of protons bounded to the observed carbon atom, ω_C and ω_H are the Larmor frequencies for the carbon and the proton, respectively, γ_C and γ_H are the corresponding gyromagnetic ratios, $\hbar$ is the Planck's constant, and r_{CH} is the carbon−proton internuclear distance, which for PVME was taken $r_{CH} = 1.09$ Å.[40]

e. Evaluation of the QENS Spectra. In the case of QENS measurements the situation is slightly different since, as for any scattering technique, we have the momentum transfer Q as an additional variable. As can be seen in Figure 5, the dynamical features change rapidly with Q. The strong Q dependence observed for the segmental dynamics of polymer melts, and glass-forming systems in general, has been interpreted as being due to the fact that the segmental dynamics in polymer melts corresponds to an anomalous diffusion process,[41,42] in which the mean-squared displacement of the main-chain protons is sublinear in time, i.e., $\langle r^2(t)\rangle \propto t^{\beta}$. Taking this into account, the normalized incoherent intermediate scattering function of the homopolymer $I_H(Q,t)$ can be expressed as

$$I_H(Q,t) = f(Q) \exp(-Q^{2x} C t^{\beta}) \tag{12}$$

where C is related to the segmental diffusivity, hence accounting for the temperature dependence, the exponent x is an empirical parameter which takes the value 1 in the Gaussian approximation, and the prefactor $f(Q)$ accounts for the missing intensity associated with the dynamics of the methyl groups. In the temperature range investigated and with the spectrometers used, $f(Q)$ can be taken as time independent because, as shown above, the methyl group motion is much faster than the segmental dynamics. Since we have three main-chain hydrogen atoms per each methyl group, and taking into account the elastic incoherent structure factor for the 3-fold methyl group rotation,[31] one finds $f(Q) = {}^1/_2[1 + (1 + 2j_0(Qr)/3)]$, j_0 being the zero-order spherical Bessel function and $r = 1.78$ Å the hydrogen−hydrogen distance in the methyl group. In the Gaussian approximation ($x = 1$) eq 12 can be rewritten as

$$I_H(Q,t) = f(Q) \exp\left[-\left(\frac{t}{C^{-1/\beta} Q^{-2/\beta}}\right)^{\beta}\right] \tag{13}$$

which has the KWW form, with a relaxation time depending on Q as $\tau(Q) = \tau_1 Q^{-2/\beta}$, $\tau_1 = C^{-1/\beta}$ being the value of the relaxation time at $Q = 1$ Å^{-1}. The scattering function of pure PVME could be described by convoluting the Fourier transform of $I_H(Q,t)$. However, to be consistent with the analysis of dielectric and NMR data, we preferred to evaluate the scattering function of pure PVME, $S_H(Q,\omega)$, as

$$S_H(Q,\omega) \propto f(Q) \frac{1}{\omega} \mathrm{Im}[-\Phi_H^*(\omega)] \otimes R(Q,\omega) \tag{14}$$

where now $\Phi_H^*(\omega)$ is Q dependent through the Q dependence of ω_P ($1/\omega_P \sim \tau(Q)$), and the model function has to be convoluted with the resolution function, $R(Q,\omega)$, of the spectrometer ($\otimes$ stands for the convolution integral). Therefore, to describe the segmental dynamics of a polymer melt as observed by means of QENS measurements, in the Gaussian approximation there are only two independent dynamical parameters, β and τ_1, accounting for the dependence on both the momentum transfer and the time/frequency. In the same framework of the analysis as for the dielectric and NMR data, it will be assumed that only τ_1 is modified by blending; hence, for the analysis of the blend data β will be taken from pure PVME, and the dynamics of the PVME segments in the blends will be characterized by the distributions $g(\log \tau_1)$. Taking this into account, the normalized QENS relaxation function corresponding to the dynamics of PVME in the blends is given in the time domain by

$$\varphi_B(Q,t) = \int_{-\infty}^{\infty} g(\log \tau_1) \exp\left[-\left(\frac{t}{\tau_1 Q^{-2/\beta}}\right)^{\beta}\right] \mathrm{d}(\log \tau_1) \tag{15}$$

and in frequency domain by

$$\Phi_B^*(Q,\omega) = \int_{-\infty}^{\infty} g(\log \tau_1) \frac{1}{\{1 + [\mathrm{i} Q^{-2/\beta} \omega/\omega_{P1}]^{\alpha}\}^{\gamma(\alpha)}} \mathrm{d}(\log \tau_1) \tag{16}$$

$\omega_{p1} = \omega_p(Q{=}1\ \text{Å}^{-1})$ being related to τ_1 by eq 6.

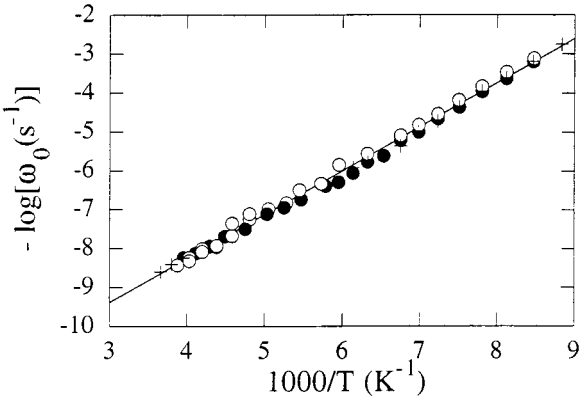

Figure 6. Temperature dependence of the characteristic frequency of the dielectric secondary relaxation process in PVME (○), PVME65 (●), and PVME50 (+). The solid line represents the fitting of the data according to an activated process.

In the blends, the contribution of dPS to the total scattering, although it is rather small (about 5% for PVME65 and 10% for PVME50), cannot be neglected. However, by comparing the spectra of the partial deuterated samples with the ones measured on fully protonated blends, we found that the dPS contribution is purely elastic for the two blends in the temperature range investigated. Therefore, in the blends we will have

$$S_B(Q,\omega) \propto \left\{c_{dPS}\delta(\omega) + (1 - c_{dPS})f(Q)\frac{1}{\omega}\,\mathrm{Im}[-\Phi_B^*(Q,\omega)]\right\} \otimes R(Q,\omega) \quad (17)$$

where $\delta(\omega)$ is the delta function accounting for the dPS contribution and c_{dPS} is the fraction of the scattering intensity coming from the dPS segments. c_{dPS} would generally be Q dependent, but due to the small dPS contribution present in the samples investigated, we have taken an average value independent of Q: $c_{dPS} = 0.05$ for PVME65 and $c_{dPS} = 0.10$ for PVME65.

V. Phenomenological Description

In this section, we present the results obtained when the evaluation method described above is used for the analysis of the experimental data shown in section III. First of all, we will depict the results obtained from the dielectric relaxation analysis where the fitting procedure is performed with all the parameters allowed to vary. However, due to the limited frequency range covered by NMR or QENS techniques, in the analysis of these data the fitting parameter characterizing the asymmetry of $g(\log \tau)$ will be fixed to the value determined from the DR data analysis.

a. Dielectric Relaxation. As commented above, before analyzing the segmental dynamics as observed by using DR, one has to characterize the dielectric secondary relaxation process. Therefore, by means of eq 1 we have fitted the dielectric relaxation data in the secondary relaxation range below T_g for PVME and the PVME65 and PVME50 blends (see solid lines in Figure 2). The thus obtained temperature dependence of ω_0 is shown in Figure 6. For all the three samples the temperature dependence of ω_0 is well described by the same Arrhenius equation (eq 2) with $E_0 = 21.7$ kJ/mol. Furthermore, the values of σ_E and $\Delta\epsilon_2$ resulted to be nearly T-independent for the three samples, and the average values found are $\sigma_E = 4.9 \pm 0.2$ kJ/mol and $\Delta\epsilon_2 = 0.12 \pm 0.01$ for pure PVME, $\sigma_E = 5.0 \pm 0.2$ kJ/mol and $\Delta\epsilon_2 = 0.08 \pm 0.01$ for PVME65, and $\sigma_E = 5.3 \pm 0.2$ kJ/mol and $\Delta\epsilon_2 = 0.06 \pm 0.01$ for PVME50. These results confirm again that within experimental uncertainties blending affects neither the characteristic frequency of the dielectric secondary relaxation process nor the shape. Also, in agreement with this result, the strength of the secondary relaxation is nearly proportional to the concentration of PVME segments in the samples. A similar result showing no dependence of the secondary relaxation on blending has recently been obtained by QENS for the secondary relaxation of poly(vinyl ethylene) component in a blend with polyisoprene.[26] Note that in this blend poly(vinyl ethylene) is the component having higher T_g. These results on polymer blends are opposite to those obtained in other two-component polymeric systems such as the case of plasticized polymers and polymer solutions. In such systems the secondary relaxation of the polymer is drastically modified by the presence of the low molecular weight component.[43]

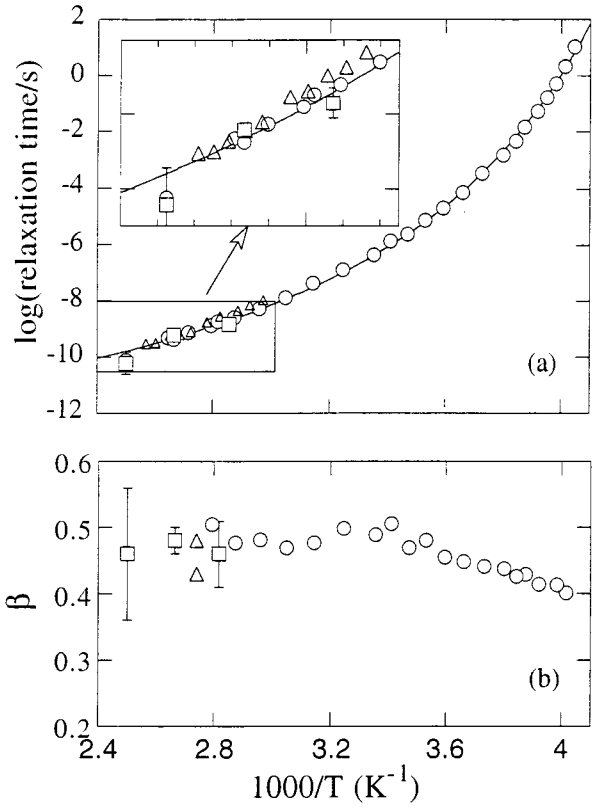

Figure 7. Temperature dependence of the KWW parameters, τ (a) and β (b), describing the segmental dynamics of pure PVME as observed by DR (circles), ^{13}C NMR (triangles), and QENS at $Q = 0.86$ Å^{-1} (squares). The solid line corresponds to a description of the data by means of the VF equation.

For the analysis of the dynamics of PVME segments as investigated by DR in pure PVME and in the blends, the values of ω_0 were extrapolated according to the Arrhenius equation (eq 2), with σ_E and $\Delta\epsilon_2$ fixed to the average values given above. Following this procedure, first, the high-temperature ($T > T_g$) experimental data of pure PVME were fitted by means of eqs 4 and 9 (see lines in Figure 1a), which implies only three fitting parameters at each temperature. The resulting values for τ and β are shown in Figure 7 as a function of reciprocal temperature. The exponent β shows a weak

temperature dependence and seems to approach a limiting value of about 0.5 at high temperatures. This limiting value is achieved in the temperature range where the secondary and the segmental relaxations seem to merge. Concerning the relaxation time τ, we found that $\tau(T)$ follows the usual non-Arrhenius temperature dependence which has been fitted by means of the Vogel−Fulcher (VF) equation, which is commonly used to describe the temperature dependence of the segmental dynamics. The VF equation reads as

$$\tau(T) = \tau_\infty \exp\left(\frac{B}{T - T_0}\right) \tag{18}$$

The values obtained for the VF parameters are shown in Table 1.

For the analysis of the DR data of the blends, we need to select a given functional form for $g(\log \tau)$. By using a generalized inverse Laplace transformation (ILT) method,[44] we have found (see Appendix) that an appropriate function for $g(\log \tau)$ is

$$g(\log \tau) \propto \left[\frac{\log(\tau/\tau_{min})}{\langle \log(\tau/\tau_{min})\rangle}\right]^{m-1} \exp\left[-m\,\frac{\log(\tau/\tau_{min})}{\langle \log(\tau/\tau_{min})\rangle}\right] \tag{19}$$

which has an average value $\langle \log \tau \rangle$ and a variance

$$\sigma^2 = \frac{(\langle \log \tau \rangle - \log \tau_{min})^2}{m} \tag{20}$$

In eq 19, which is obtained from a χ^2 distribution[45] (see Appendix), m is a measure of the symmetry of the distribution shape (for $m \gg 1$ it corresponds to a symmetric Gaussian distribution) and τ_{min} is the fastest relaxation time in the distribution. Thus, for fitting the dielectric experimental data of the two blends in the whole temperature range, we have combined eqs 8, 9, and 19. In this way the three parameters that determine the distribution function, m, σ, and $\langle \log \tau \rangle$, can be extracted by fitting the dielectric loss data using standard minimization methods. Note that in this procedure the total number of fitting parameters is four; i.e., $\Delta\epsilon_1$ is the single additional fitting parameter. In this way, it is found that the shape of the relaxation patterns from the blends is very well described (see Figure 1b,c). The resulting values of $\langle \log \tau \rangle$ and σ are shown in Figures 8 and 9, respectively. As can be seen, we found a non-Arrhenius temperature dependence of the average value $\langle \log \tau \rangle$ and a rapid narrowing of the distribution $g(\log \tau)$ as the temperature increases (the variance reduces dramatically). To illustrate this behavior, some representative $g(\log \tau)$ curves constructed with the fitting parameters obtained for PVME65 are depicted in Figure 10a. In this figure it is apparent that as the temperature increases, $g(\log \tau)$ also becomes more and more asymmetric. This latter finding is associated with the fact that whereas at low temperatures, close to T_g, the values of m are large, and hence $g(\log \tau)$ is Gaussian-like (see Figure 10a), at high temperatures the value of m becomes rather low, approaching a limiting value of $m = 2$. It should also be mentioned that the Gaussian-like distribution of $\log \tau$, close to T_g, is in agreement with previous results obtained in this temperature range on the same blends.[2,20,21]

At high temperatures, where the distribution is very asymmetric, the values of τ_{min} reflect actually the fastest segmental dynamics present in the systems. As can be seen in Figure 8, the values of τ_{min} in this range are close to the relaxation times of the segmental dynamics of pure PVME at the same temperature, which is meaningful. On the contrary, close to T_g, $g(\log \tau)$ is rather symmetric, and the obtained τ_{min} values become meaningless. This is illustrated in Figure 10a for PVME65 at $T = 273$ K, where the obtained value of τ_{min}, which is of the order of 10^{-12} s, is far apart from the range where $g(\log \tau)$ takes significant values. Nevertheless, in that temperature range one can define an effective value of τ_{min} by extrapolating linearly the low τ behavior of $g(\log \tau)$ as shown in the inset of Figure 10a. (The same linear extrapolation at high temperatures would yield the actual value of τ_{min}.) The values thus obtained are depicted in Figure 8 as pluses. As can be seen in Figure 8, at high temperatures the so-obtained values of τ_{min} coincide with the relaxation times of pure PVME; however at temperatures close to T_g, τ_{min} seems to become systematically shorter than the τ values of PVME. It should be noted that the description of the data in this temperature range by fixing the value of τ_{min} to the one of pure PVME, and allowing the other parameters to vary freely, is not good in the low-

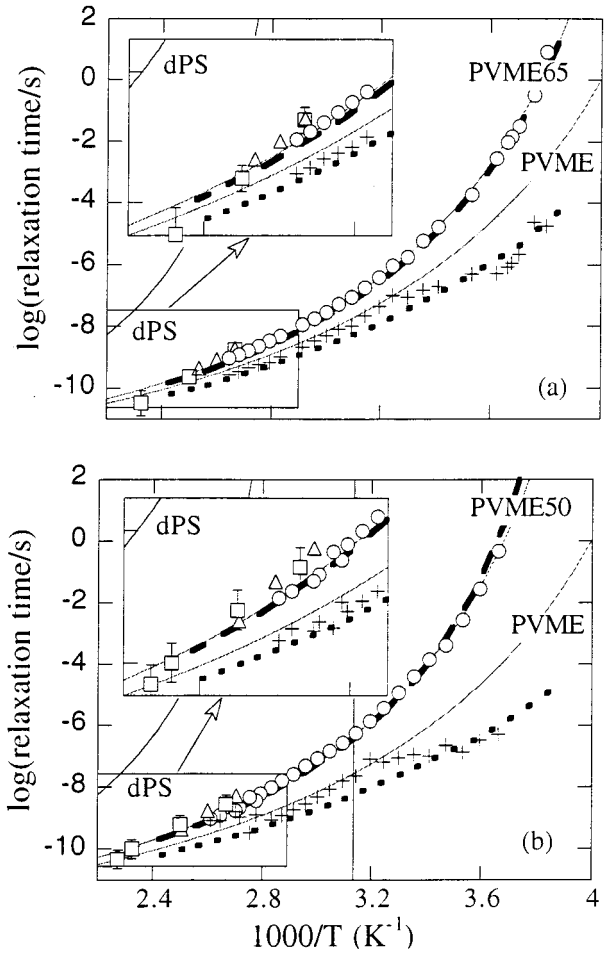

Figure 8. Temperature dependence of the average relaxation time of the dynamics of the PVME segments in the blends: (a) PVME65; (b) PVME50, as observed by DR (circles), ^{13}C NMR (triangles), and QENS at $Q = 0.86$ Å^{-1} (squares). The values of the minimum relaxation times in the distribution obtained from DR measurements are also included as crosses. The solid lines correspond to a description of the data of the components and the blends by means of a VF equation. The thick dashed ($\langle \log \tau \rangle$) and dotted ($\tau_{min}$) lines correspond to the values obtained when a temperature-independent Gaussian distribution of T_0 is assumed.

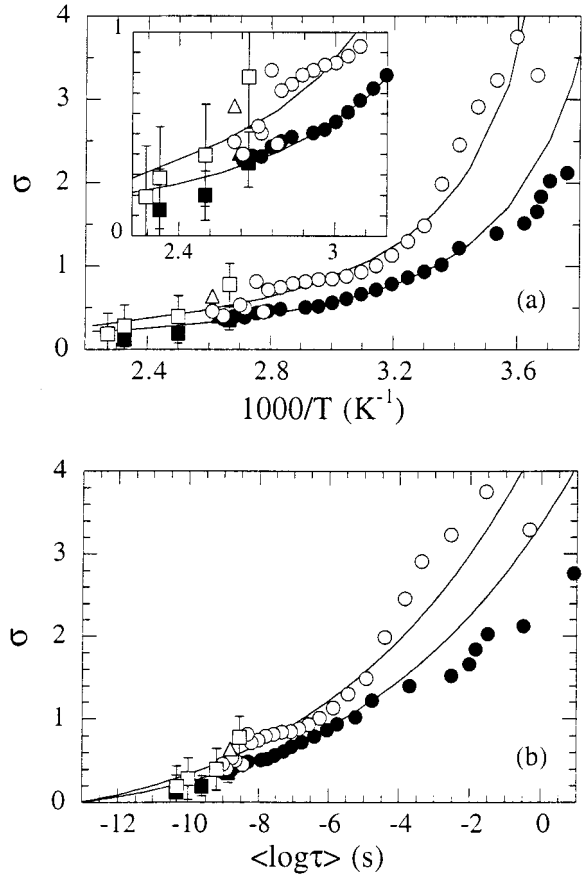

Figure 9. (a) Temperature dependence of the square root of the variance of the distribution of KWW relaxation times describing the dynamics of the PVME segments in the blends, PVME65 (empty symbols) and PVME50 (filled symbols), as observed by DR (circles), ^{13}C NMR (triangles), and QENS (squares). The solid lines correspond to the values obtained when a temperature-independent Gaussian distribution of T_0 is assumed. In (b) the same data are plotted as a function of the corresponding average values of the relaxation time.

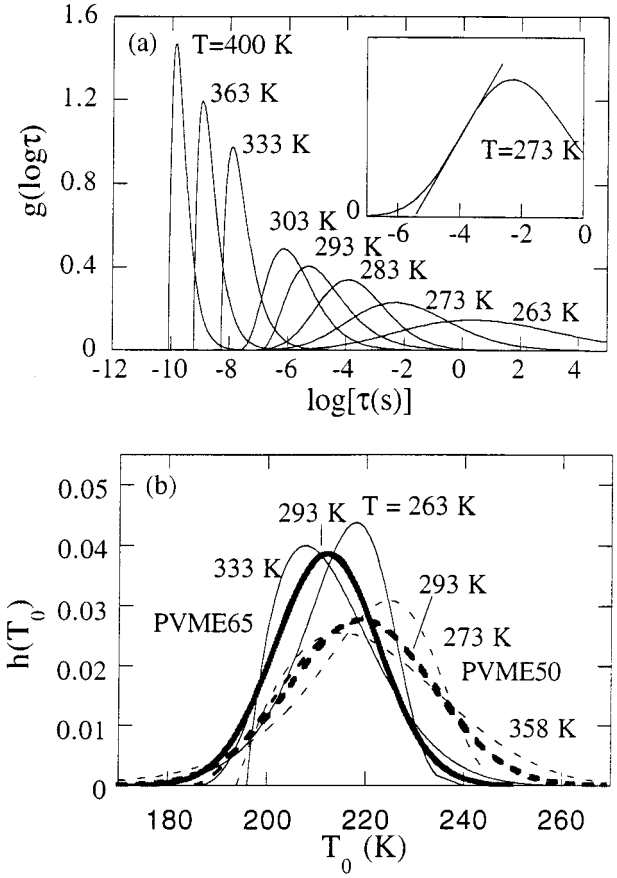

Figure 10. (a) Representative distributions of the KWW relaxation times $g(\log \tau)$ describing the dynamics of the PVME segments in the PVME 65 blend at several temperatures. The inset is a magnification of the 293 K curve showing how τ_{min} is determined for distributions with $m > 2$. In (b) some of the distributions of T_0 values obtained from $g(\log \tau)$ for PVME65 (solid lines) and PVME50 (dashed lines). The thick lines show Gaussian functions fitting the $h(T_0)$ distributions at 293 K for the two blends.

temperature range (see Figure 11). This would mean that, at least close to T_g, the dynamics of some PVME segments in the blend is faster than the one found in pure PVME. A possible interpretation of this result is that the lack of packing of dPS and PVME might allow regions with a "free volume" greater than the one in pure PVME.

b. Nuclear Magnetic Resonance and Quasielastic Neutron Scattering. Once the dielectric data have been analyzed, by using the same analysis procedure we now check whether the results from other experimental techniques render a consistent picture of the dynamics of the PVME segments and the effect of blending. For the analysis of the ^{13}C NMR and the QENS data in the blend the value of m in eq 19 was fixed to $m = 2$. This value was determined from the DR analysis at high temperatures ($T > 310$ K). It should be noted that a direct determination of m by these techniques is impossible since they cover a rather narrow frequency range.

1. Nuclear Magnetic Resonance. As previously mentioned, the ^{13}C NMR data of pure PVME were analyzed on the basis of a dipolar mechanism for the magnetic moment relaxation. First, the values for α in eq 4 were determined from the experimental values of T_{1min}. This is only possible when a relaxation function with a single temperature-independent shape parameter is assumed,

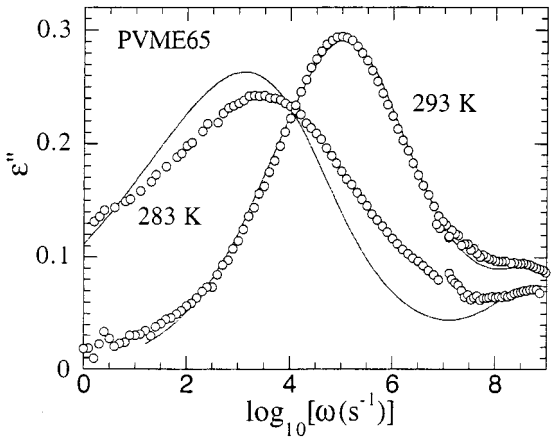

Figure 11. Fitting of some dielectric relaxation data of the PVME 65 blend by fixing the value of τ_{min} to the one corresponding to pure PVME.

as we do, to describe the C−H bond reorientation. The thus-obtained values of β for the CH and CH_2 carbons are shown in Figure 7b. It is found that both are close to those obtained by DR. However, the value corresponding to the CH carbons seems to match better the DR results. These differences could indicate that the C−H bond reorientation is slightly affected by other dynamical processes different from the segmental dy-

namics, this effect being more pronounced for the CH_2 carbons.

For the analysis of the T_1 data in the blend, the values of α (β) obtained in pure PVME were fixed. Since the value of m was also fixed to $m = 2$, the variance of the $g(\log \tau)$ distribution is the single free parameter for its shape. Moreover, the dielectric results show that σ changes moderately in the temperature range around the minima of T_1, and as a first approximation, it can be taken as a constant. This assumption allows to calculate the values for σ which account for the experimental values of $T_{1\min}$ in the blends, by using eqs 8 and 10. As can be seen in Figure 9, the resulting values, which were indistinguishable for the two main-chain carbons in each blend composition, agree very well with those obtained by fitting the DR data of the blends.

On the other hand, once the shape of the relaxation functions have been obtained for the three samples, the relevant time scale is the single parameter determining the values of T_1 in eq 10. Therefore, from the respective experimental values of T_1, the values of τ in pure PVME and $\langle \log \tau \rangle$ in the blends were determined directly by using eq 10. The results thus obtained for PVME are shown in Figure 7a. A good agreement between the NMR and DR results is apparent (see inset of Figure 7a). For the blends, due to the actual temperature dependence of σ, the calculation of $\langle \log \tau \rangle$ was restricted to a few degrees around the temperature of $T_{1\min}$. In this way, it is found that also for the blends the agreement between the NMR and DR relaxation times is very good (see Figure 8).

2. Quasielastic Neutron Scattering. The QENS data of pure PVME and the blends were analyzed by means of eqs 14 and 17, respectively. For pure PVME the parameters β and τ_1 at 350, 375, and 400 K were obtained at each temperature by a simultaneous fitting of the QENS spectra corresponding to different Q values (see solid lines in Figure 5a as representative curve fittings). The resulting values for β, which are determined with a rather high uncertainty mainly at 400 K, are shown in Figure 7b. A good agreement of the QENS β values and those obtained by DR and ^{13}C NMR is again apparent. Concerning the relaxation times, when comparing the values obtained from relaxation techniques with those determined from scattering measurements, the Q dependence of the latter needs to be taken into account. Since in our case this Q dependence is assumed to be a power law, it is always possible to find a Q value for which the relaxation time determined from scattering measurements at a given temperature equals that found by means of relaxation techniques. As can be seen in Figure 7a, for pure PVME a Q value of 0.86 $Å^{-1}$ allows at each temperature a rather good matching between the QENS relaxation times and those obtained by using relaxation techniques. Although at the highest temperature a slightly lower Q value would provide a better agreement, within the experimental uncertainties involved the agreement found is good. It is noteworthy that the Q value for which the QENS times agree with the ones determined from DR and ^{13}C NMR is in the Q range covered experimentally, and therefore it is hardly sensitive to the particular Q dependence of τ assumed in the data analysis.

For the analysis of the QENS spectra of the blends an average $\beta = 0.48$ was used at all the temperatures. Thus, the QENS spectra of the blends corresponding to different Q values were fitted simultaneously at each temperature by means of eqs 16 and 17 to obtain $\langle \log \tau_1 \rangle$ and σ (assuming again $m = 2$ in eq 19). The solid lines in Figure 5b show some representative curve fitting. As shown in Figure 9, the thus-obtained values of σ also agree well with those determined from the relaxation techniques. Moreover, it is found that the values of $\langle \log \tau \rangle$ for the blends, at the same Q value used for PVME ($Q = 0.86$ $Å^{-1}$), also yield a good agreement between the QENS and the DR and NMR values (see Figure 8).

VI. Discussion

The main assumption of the analysis for the α-relaxation described above is that the dynamics of the PVME segments in the blends is a simple superposition of processes, each of which has the shape of the segmental process in pure PVME. In the phenomenological description we have found that this simple picture is able to account consistently for the dynamics of the PVME segments in the blends as observed by three different experimental techniques. In particular, in the two blends investigated here, the different experimental techniques yield the same values of the dynamical parameters evaluated. It was reported previously,[28] and confirmed here, that the segmental dynamics of pure PVME as observed by different experimental techniques may be described consistently. Our results in this work evidence that this characteristic is not lost by blending. Furthermore, the value of Q for which the QENS time scale matches the scale of the relaxation techniques is, for the two blends investigated, identical to that found for pure PVME.

An important problem which remains to be addressed is the origin of the relaxation time distribution. To gain more insight into this question, we have analyzed the temperature dependence of the evaluated dynamical parameters. First, we have fitted the $\langle \log \tau \rangle$ values of the blends by means of the VF equation (eq 18). The obtained parameters are shown in Table 1, and the corresponding temperature laws are displayed in Figure 8. It was found that, within the experimental uncertainties, τ_∞ and B were the same in pure PVME and in the two blends. Thus, it seems that T_0 is the only parameter of eq 18 that is actually modified by blending. On the basis of the result that B and τ_∞ are not modified by blending, the distribution of T_0 values responsible for the relaxation time distribution $g(\log \tau)$ can be calculated as

$$h(T_0) = g(\log \tau)\frac{\mathrm{d} \log \tau}{\mathrm{d}T_0} = g(\log \tau)\frac{B \log \mathrm{e}}{(T - T_0)^2} \quad (21)$$

The such-obtained $h(T_0)$ distributions at several temperatures are shown in Figure 10b. As can be seen, the resulting distributions for each blend composition are weakly dependent on temperature with similar average T_0 values. At intermediate temperatures $h(T_0)$ is rather symmetric and can be very well described by using Gaussian functions (see the thick lines in Figures 10b) with the values of the average and the variance shown in Table 1. Note that around this temperature range (293 K) the relaxation process is well centered in the experimental frequency window for the two blends, and therefore the possible cutoff effects should be weak. However, at lower and higher temperatures, the obtained distributions $h(T_0)$ can certainly be affected by these effects. Thus, despite the apparent changes of

$h(T_0)$ with temperature, it is not clear whether these changes are genuine or whether they are due to the experimental uncertainties and cutoff effects. To investigate this question further, we have calculated the distributions $g(\log \tau)$ at several temperatures, for each blend composition, assuming that $h(T_0)$ does not depend on temperature, i.e., $h(T_0)$ is taken as the Gaussian distribution found at 293 K. From these distributions we have evaluated $\langle \log \tau \rangle$, σ, and $\log \tau_{min}$, the latter following the same geometrical construction used before. A good agreement between the phenomenological values of $\langle \log \tau \rangle$ with those deduced from the temperature-independent Gaussian distribution of T_0 is found (see dashed lines in Figure 8) which extends over 150 K. It is also noteworthy that for each blend composition the Gaussian distribution extends to T_0 values significantly smaller than the one corresponding to PVME ($T_0 = 200$ K). This evidences once again the already mentioned fact that in the blends there exist processes faster than those in pure PVME. The reasonable agreement between the experimental values of $\log \tau_{min}$ and those deduced from a Gaussian $h(T_0)$ (see dotted lines in Figure 8) shows that this tail of the Gaussian function is relevant in order to account for the dynamics of the PVME segments in the blends. The contribution of these processes can be estimated to be of about 12% for PVME65 and 10% for PVME50. Despite the agreement found with this assumption, in Figure 9a it is also apparent that the temperature dependence of the variance shows small but significant discrepancies in the two blends below ca. 277 K. It is noteworthy that nonequilibrium effects are expected to occur in this temperature range.[46] In fact, we have found that a temperature-independent distribution $h(T_0)$ allows to account for the main features of the experimental dielectric relaxation of the blends at the temperatures around and above that of the inflection point of the DSC trace whereas at lower temperatures $h(T_0)$ should change.[47,48]

The interpretation of the previously reported dielectric relaxation results in PVME/PS blends[20,21] was based on the assumption that as a consequence of CF the glass transition temperature is different in different subvolumes. These different glass transition temperatures yield, through the Williams−Landel−Ferry equation,[32] a distribution of relaxation times. This approach implies that at a given concentration the dynamics of the α-relaxation in the blend can be described by a single glass transition temperature. In this picture all the parameters of eq 18 should change with blending from those of pure PVME ($\tau_\infty = 9 \times 10^{-14}$ s, $B = 1505$ K, $T_0 = 200$ K) to those of pure PS ($\tau_\infty = 3 \times 10^{-13}$ s, $B = 1272$ K, $T_0 = 326$ K). Our data do not support this view, since B and τ_∞ remain unaffected by blending. Moreover, the value of T_0 hardly extrapolates to the PS value in the limit of zero PVME content. Furthermore, if B and τ_∞ remain unaffected by blending, at very high temperatures the dynamics of the PVME segments in the blends would result indistinguishable from that in pure PVME, and hence σ should extrapolate to zero at high temperatures. As shown in Figure 9, this is compatible with our experimental findings since in the high-temperature limit (relaxation times close to $\tau_\infty \cong 10^{-13}$ s in Figure 9b) σ actually extrapolates to zero.

The above findings may be illustrated in more detail by the following considerations: Let us define the glass transition temperature in the usual way as the temperature where the dielectric relaxation time reaches $\tau = 1$ s. For pure PVME this criterion results in $T_g = 250$ K coinciding with the T_g taken as the inflection point of the DSC curve. From Figure 8 we may now read off corresponding T_g values for 50% and 65% PVME content in the blend, yielding $T_g = 272$ K for PVME50 and 267 K for PVME65. We emphasize that the relaxation rates important here have directly been measured and were not extrapolated. In a similar way, one may also obtain glass transition temperatures for higher PS concentrations,[47,48] though, because of problems to reach equilibrium, extrapolations through the corresponding VF laws have to be performed. Figure 12 compares the thus-obtained T_g values from the relaxation of PVME with the DSC T_g's from the identical blends, again taken from the inflection points. At low PS content both temperatures are similar, but already at 50% PS a significant difference of $\Delta T_g = 10$ K beyond any experimental error is observed. It is worth emphasizing once again that, for this concentration, we compare measured, and not extrapolated, quantities. If we go further in dPS concentration, the discrepancies increase and reach ΔT_g around 60 K at 80% PS.[47,48] These results demonstrate that, in the blend, PVME keeps its individuality as suggested by the observation of constant Vogel−Fulcher parameters B and τ_∞ with blending. Thus, the segmental dynamics of different polymers in the blend lead to different glass transition temperatures for each polymer, implying that the concept of a single T_g related to the actual concentration within a CF must be invalid. Dynamically, there does not exist a common T_g for both polymers at a certain concentration. From that result it stands that, if each polymer, even at T_g, keeps its individuality in exhibiting very different segmental relaxation rates, then in a well-miscible system the concept of cooperatively relaxing regions has at least to be rethought. Further experiments on well-miscible systems where both components can be accessed dielectrically will give more detailed insight into this problem.

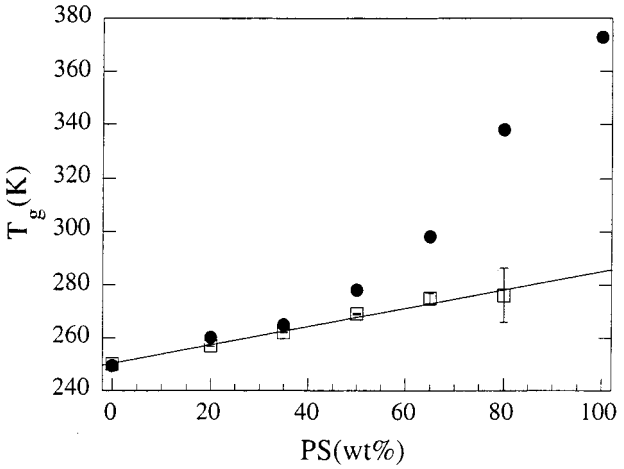

Figure 12. Comparison between the glass transition temperatures of the PVME/dPS blends obtained form DSC (filled symbols) and from the average relaxation time representing the dynamics of the PVME segments in the blend (empty symbols).

VII. Conclusions

We have studied the dynamics of the PVME segments in two blend compositions of PVME and dPS by using three different experimental techniques—DR, NMR, and QENS—and covering a wide range in the time/frequency

scale. Two main relaxation processes are observed in this range: the secondary β-relaxation and the segmental α-relaxation. Our findings show that the localized motions involved in the β-relaxation are not affected by blending. On the other hand, we have found that the results obtained for the α-relaxation can be consistently described in terms of a simple superposition of PVME-like processes, i.e., by relaxation processes which are described by a KWW function with the β exponent found for pure PVME. The relaxation time distributions for the PVME segments of the blends are well accounted for by means of a χ^2-type distribution function. The relaxation times corresponding to the average of the distributions follow a VF equation, T_0 being the single parameter affected by blending. In agreement with this result, the variance of the distribution of relaxation times vanishes in the high-temperature limit. It has also been shown that, in the temperature range above the inflection point of the DSC trace of the blends, the shape and temperature dependence of the distribution of relaxation times can be accounted for by a temperature-independent Gaussian distribution of T_0. This distribution shows an average value and variance which increase with decreasing PVME content. Furthermore, for T_0 values smaller than that of PVME these distributions still persist, which implies that a significant number of PVME segments in the blends move faster than in pure PVME. This should indicate a lack of dense packing of the PVME segments, likely due to the presence of the more stiff PS chains. Finally, the present results strongly indicate that each polymer component of the blend exhibits very different segmental relaxation rates, i.e., different "glass transitions". This result seems to be relevant not only in the framework of polymer blend dynamics but also in connection with the concept of cooperatively relaxing regions and the glass transition problem.

Acknowledgment. This work has been supported by the Spanish Ministry of Education (MEC) (projects PB94-0468 and PB97-0638), the Government of the Basque Country (project GV-PI98/20), and the University of the Basque Country (projects 206.215-G20/98). A.A., I.C., J.M.A., and J.C. thank Gipuzkoako Foru Aldundia and Iberdrola S.A. for partial financial support. I.C. thanks the grant of the Basque Government. The facilities given by ILL are also acknowledged. Dr. Arbe is also acknowledged for computing assistance with DISCUS and fruitful discussions. The support from the "Donostia International Physics Center" is also acknowledged.

Appendix

For the analysis of the experimental data of the blends in the framework of the evaluation strategy used in this work, one had to choose an appropriate functional form for $g(\log \tau)$. One might try a Gaussian function, i.e.

$$g(\log \tau) = \frac{1}{\sqrt{2\pi}\sigma} \exp\left[-\frac{(\log \tau - \langle \log \tau \rangle)^2}{2\sigma^2}\right]$$

where $\langle \log \tau \rangle$ corresponds to the average relaxation time and σ^2 to the variance. However, this type of distribution fails to describe the dielectric data well (see dashed line in Figure 13 as an example). Alternatively, instead of imposing a given functional form of the distribution of relaxation times, in favorable situations (i.e., when the relaxation process of interest is well centered in a broad frequency window and does not overlap very much with other processes), it is possible to obtain the distribution function directly from the experimental data by solving eq 8 with a generalized inverse Laplace transformation (ILT) method.[44] For the blends investigated here this is only possible in a very narrow temperature range (around 293 K) of the DR measurements. At lower temperatures the slower part of the segmental dynamics is clearly out of the experimental window, and at high temperatures the segmental dynamics and the secondary relaxation processes overlap very much (see Figure 1b,c). Thus, we have applied the ILT method to the PVME65 dielectric data at 293 K after the subtraction of the secondary relaxation contribution (see Figure 13). The resulting $g(\log \tau)$ is depicted in Figure 14. We have found that such a distribution function can be well described starting from a χ^2-distribution function if a convenient change of the variable is made. The χ^2-distribution function can be written as[45]

$$g(y) = \frac{1}{2^m \Gamma(m)} \left[\frac{y}{2}\right]^{m-1} \exp\left(-\frac{y}{2}\right)$$

This equation is defined for a positive statistical variable y, $0 \le y < \infty$, having an average value $\langle y \rangle = 2m$ and a

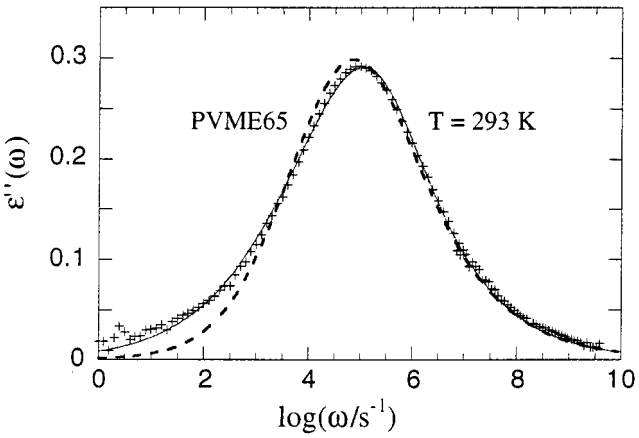

Figure 13. Dielectric data from PVME65 at 293 K once subtracted from the secondary relaxation contribution. The dashed line represents the best fit assuming a Gaussian form for $g(\log \tau)$ and the solid line the one obtained by using a χ^2-type $g(\log \tau)$ distribution.

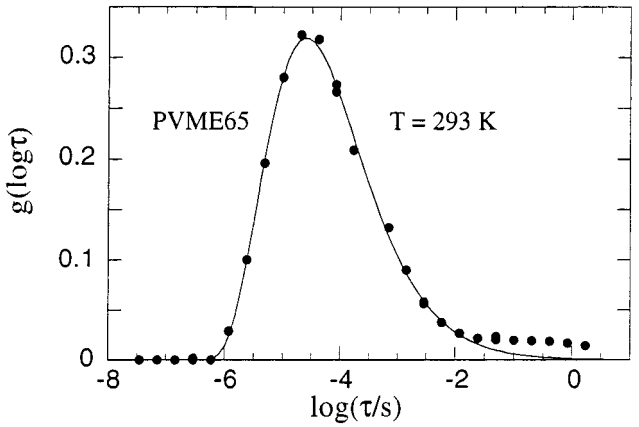

Figure 14. Distribution of relaxation times $g(\log \tau)$ (points) obtained directly from the data shown in (A) using a generalized inverse Lapace transformation method. The line is the fit with a χ^2-type $g(\log \tau)$ distribution.

variance $4m$. To use this functional form for describing the obtained $g(\log \tau)$ distribution, the variable y can be defined as $y = 2m \log(\tau/\tau_{min})/\langle\log(\tau/\tau_{min})\rangle$. Thus, $g(\log \tau)$ can be written as

$$g(\log \tau) = \frac{1}{\langle\log(\tau/\tau_{min})\rangle} \frac{m^m}{\Gamma(m)} \times \left[\frac{\log(\tau/\tau_{min})}{\langle\log(\tau/\tau_{min})\rangle}\right]^{m-1} \exp\left[-m \frac{\log(\tau/\tau_{min})}{\langle\log(\tau/\tau_{min})\rangle}\right]$$

As shown in Figure 14, this equation allows a good description of the distribution determined directly from the experimental data of PVME65 at 293 K.

References and Notes

(1) Wetton, R. E.; MacKnight, W. J.; Fried, J. R.; Karasz, F. E. *Macromolecules* **1978**, *11*, 158. Shears, M. S.; Williams, G. *J. Chem. Soc., Faraday Trans. 2* **1973**, *69*, 608.
(2) Zetsche, A.; Kremer, F.; Jung, W.; Schulze, H. *Polymer* **1990**, *31*, 1883.
(3) Roland, C. M.; Ngai, K. L. *Macromolecules* **1991**, *24*, 2261, 5315.
(4) Alegría, A.; Colmenero, J.; Ngai, K. L.; Roland, C. M. *Macromolecules* **1994**, *27*, 4486.
(5) Chung, G.-C.; Kornfield, J. A.; Smith, S. D. *Macromolecules* **1994**, *27*, 964, 5729.
(6) Katana, G.; Fischer, E. W.; Hack, T.; Abetz, V.; Kremer, F. *Macromolecules* **1995**, *28*, 2714.
(7) Mansour, A. A.; Madbouly, S. A. *Polym. Int.* **1995**, *36*, 269; **1995**, *37*, 267.
(8) Zhao, J.; Chin, Y. H.; Liu, Y.; Jones, A. A.; Inglefield, P. T.; Kambour, R. P.; White, D. M. *Macromolecules* **1995**, *28*, 3881.
(9) Arrighi, V.; Higgins, J. S.; Burgess, A. N.; Howells, W. S. *Macromolecules* **1995**, *28*, 4622.
(10) Alegría, A.; Elizetxea, C.; Cendoya, I.; Colmenero, J. *Macromolecules* **1995**, *28*, 8819.
(11) Goodwin, A.; Marsh, R. *Macromol. Rapid Commun.* **1996**, *17*, 475.
(12) Flores, R.; Perez, J.; Cassagnau, P.; Michel, A.; Cavaille, J. Y. *J. Appl. Polym. Sci.* **1996**, *60*, 1439.
(13) Mansour, A. A. *Polym. Int.* **1997**, *43*, 70.
(14) Bershtein, V. A.; Egorova, L. M.; Prudhomme, R. E. *J. Macromol. Sci. Phys.* **1997**, *36*, 513.
(15) Arendt, B. H.; Krishnamoorti, R.; Kornfield, J. A.; Smith, S. D. *Macromolecules* **1997**, *30*, 1127.
(16) Alegría, A.; Cendoya, I.; Colmenero, J.; Alberdi, J. M.; Frick, B. *Physica A* **1997**, *234*−*236*, 442.
(17) Mukhopadhyay, R.; Alegría, A.; Colmenero, J.; Frick, B. *J. Non-Cryst. Solids* **1998**, *235*−*237*, 233.
(18) Karatasos, K.; Vlachos, G.; Vlassopoulos, D.; Fytas, G.; Meier, G.; DuChesne, A. *J. Chem. Phys.* **1998**, *108*, 5997.
(19) Peng, Z. L.; Olson, B. G.; Srithawatpong, R.; McGervey, J. D.; Jamieson, A. M.; Ishida, H.; Meier, T. M.; Halasa, A. F. *J. Polym. Sci., Part B: Polym. Phys.* **1998**, *36*, 861.
(20) Fischer, E. W.; Zetsche, A. *ACS Polym. Prepr.* **1992**, *33*, 78.
(21) Zetsche, A.; Fischer, E. W. *Acta Polym.* **1994**, *45*, 168.
(22) Sanat, K. K.; Colby, R. H.; Anastasiadis, S. H.; Fytas, G. *J. Chem. Phys.* **1996**, *105*, 3777.
(23) Roland, C. M.; Ngai, K. L. *Macromolecules* **1992**, *25*, 363.
(24) Alegría, A.; Colmenero, J.; Mari, P. O.; Campbell, I. A. *Phys. Rev. E* **1999**, *59* (June 1).
(25) Alvarez, F.; Alegría, A.; Colmenero, J. *Macromolecules* **1997**, *30*, 597.
(26) Arbe, A.; Alegría, A.; Colmenero, J.; Hoffmann, S.; Willner, L.; Richter, D. *Macromolecules*, submitted.
(27) Kumar, S. K.; Colby, R. H.; Anastiasadis, S. H.; Fytas, G. *J. Chem. Phys.* **1996**, *105*, 3777.
(28) Colmenero, J.; Alegría, A.; Alberdi, J. M.; Alvarez, F.; Frick, B. *Phys. Rev. B* **1991**, *44*, 7321.
(29) Yang, H.; Shibayama, M.; Stein, R. S.; Shimizu, N.; Hasimoto, T. *Macromolecules* **1986**, *19*, 1667.
(30) Johnson, M. W. In DISCUS: A Computer Program for the Calculation of Multiple Scattering Effects in Inelastic Neutron Scattering experiments; HARWELL HL74/1054(C13).
(31) Mukhopadhyay, R.; Alegría, A.; Colmenero, J.; Frick, B. *Macromolecules* **1998**, *31*, 3985. Chahid, A.; Alegría, A.; Colmenero, J. *Macromolecules* **1994**, *27*, 3282.
(32) McCrum, N. G.; Read, B. E.; Williams, G. *Anelastic and Dielectric Polymeric Solids*; Dover Publications: New York, 1991.
(33) Böttcher, C. J. F. *Theory of Electric Polarization*; Elsevier Scientific: Amsterdam, 1973.
(34) Williams, G. Watts, D. C. *Trans. Faraday Soc.* **1970**, *66*, 80.
(35) Alvarez, F.; Alegría, A.; Colmenero, J. *Phys. Rev. B* **1991**, *44*, 7306; **1993**, *47*, 125.
(36) Alegría, A.; Guerrica-Echevarría, E.; Goitiandía, L.; Tellería, I.; Colmenero, J. *Macromolecules* **1995**, *28*, 1516.
(37) Hofmann, A.; Alegría, A.; Colmenero, J.; Willner, L.; Buscaglia, E.; Hadjichristidis, N. *Macromolecules* **1996**, *29*, 129.
(38) Havriliak, S., Jr.; Havriliak, S. J. *Dielectric and Mechanical relaxation in Materials: Analysis, Interpretation, and Application to polymers*; Hamser Publishers: Munich, 1997.
(39) Mehring, M. *Principles of High-Resolution NMR in Solids*; Springer-Verlag: Berlin, 1983; Chapter 8.
(40) Dejean de la Batie, R.; Lauprete, F.; Monnerie, L. *Macromolecules* **1988**, *21*, 2045.
(41) Colmenero, J.; Alegría, A.; Arbe, A.; Frick, B. *Phys. Rev. Lett.* **1992**, *69*, 478.
(42) Arbe, A.; Colmenero, J.; Monkenbusch, M.; Richter, D. *Phys. Rev. Lett.* **1998**, *81*, 590. Arbe, A.; Alegría, A.; Colmenero, J.; Monkenbusch, M.; Richter, D. *J. Phys.: Condens. Matter* **1999**, *11*, A363.
(43) Maxwell, A. S.; Monnerie, L.; Ward, I. M. *Polymer* **1998**, *26*, 6851.
(44) Alvarez, F.; Alegría, A.; Colmenero, J. *J. Chem. Phys.* **1995**, *103*, 798.
(45) Carnahan, B.; Luther, H. A.; Wilkes, J. O. *Applied Numerical Methods*; Wiley: New York, 1969; p 559.
(46) Takeno, H.; Koizumi, S.; Hasegawa, H.; Hashimoto, T. *Macromolecules* **1996**, *29*, 2440.
(47) Cendoya, I. Ph.D. Thesis.
(48) Cendoya, I.; Alegría, A.; Alberdi, J. M.; Colmenero, J., to be published.

MA9819539